# Structural transitions in surface-stabilized smectic-*C* cells near the smectic-*C*–smetic-*A* phase-transition temperature

N. Vaupotič,[1,2] M. Čopič,[2,3] and T. J. Sluckin[4]
[1]*Department of Physics, Faculty of Education, University of Maribor, Koroška 160, 2000 Maribor, Slovenia*
[2]*Department of Physics, University of Ljubljana, Jadranska 19, 1111 Ljubljana, Slovenia*
[3]*Jožef Stefan Institute, University of Ljubljana, Jamova 39, 1111 Ljubljana, Slovenia*
[4]*Faculty of Mathematical Studies, University of Southampton, Southampton SO17 1BJ, United Kingdom*
(Received 9 October 1997)

This study continues the development of the Landau–de Gennes theory of chevron structure in a surface-stabilized Sm-*C* liquid crystal cell. In this paper we study in detail the consequences of varying the magnitude of the planar surface anchoring. The strength of the anchoring is found to govern the order of the phases close to the Sm-*A*–Sm-*C* phase transition. Depending on the strength of the anchoring, we find two possible transition sequences: (a) Sm-*A*→bookshelf Sm-*C*→nonplanar chevron; (b) Sm-*A*→planar chevron →nonplanar chevron. [S1063-651X(98)15705-7]

PACS number(s): 61.30.Cz, 61.30.Jf, 64.70.Md

## I. INTRODUCTION

The chevron structure is a widespread feature in surface stabilized ferroelectric Sm-*C* liquid crystal cells. It was first observed in x-ray scattering work [1,2]. Afterwards it was also confirmed by optical experiments [3–8]. The chevron structure can exist both in thin and thick sample textures [1,2,9]. It is formed when a cell, filled with Sm-*A* liquid crystal, is cooled to the Sm-*C* phase [1,2]. Usually, once the layers are formed in the Sm-*A* phase, the surface positional anchoring is frozen in and the layers do not move along the glass plates [10]. In this case the only way to maintain the periodicity of the Sm-*A* liquid crystal along the surface and reduce the layer thickness in the Sm-*C* phase simultaneously is to tilt the layers away from the normal to the bounding plates. A schematic diagram showing the bookshelf Sm-*A* and chevron Sm-*C* layer structures is given in Fig. 1.

This phenomenon has given rise to considerable theoretical interest. A number of different models of the layer and director structures in Sm-*C* chevron cells have been presented over the past ten years [11–20]. In particular, in Ref. [21], which we shall refer to as I, we used a Landau–de Gennes type model [22] to study the chevron structure.

The model presented in I involves a free energy written in covariant form, as first suggested by Lubensky and co-workers [23,24]. This model retains the conceptual simplicity of the model of Clark and co-workers [11,12], but it no longer requires many of the simplifying computational assumptions employed in other models of the chevron structure. It is also a very general and economical model, as it retains all the relevant degrees of freedom and phase transitions with a minimum number of parameters. In I, we investigated the director and the layer structure as a function of the nematic and smectic elastic constants and of the strength of the surface orientational anchoring. We were able to obtain the spatial variation of the free energy density and calculate the energy associated with the chevron wall. In this way, bistability occurs without additional assumptions. It was also possible to study the temperature dependence of the chevron structure.

Also of some interest is the temperature dependence of the chevron structure close to the Sm-*A*–Sm-*C* phase transition. We have found in I that in the case of a free surface—no orientational anchoring of the director at the surface and only strong positional anchoring of the smectic layers—the chevron structure is not formed immediately below the Sm-*A*–Sm-*C* bulk transition temperature. Rather, we found that the bookshelf Sm-*C* structure can exist in a narrow temperature region between the Sm-*A* structure and the chevron Sm-*C* structure. However, this extremely weak anchoring hypothesis is not realistic, and must be replaced by a finite anchoring condition. An important factor here is that the bookshelf Sm-*C* structure is by far the most desirable for electro-optical applications. It would therefore be

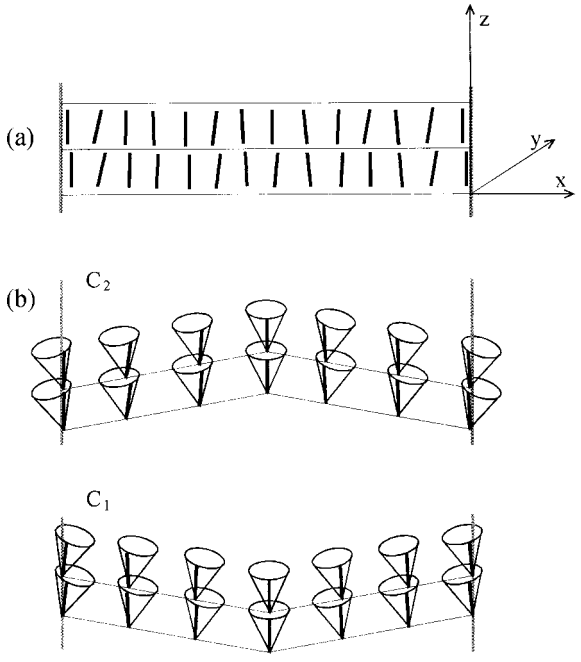


FIG. 1. Bookshelf Sm-*A* structure (a) and two types ($C_1$ and $C_2$) of the Sm-*C* chevron structure (b). The periodicity along the surface is the same in both structures.

 

useful to know how the strength and type of the surface orientational anchoring and the magnitude of the nematic and smectic elastic constants affect the temperature region over which the bookshelf structure can exist.

In this paper we continue the study which we began in I. Here we investigate the threshold conditions for the formation of the chevron and bookshelf Sm-$C$ structure close to the Sm-$A$–Sm-$C$ phase transition as a function of the surface orientational anchoring strength, which we define more precisely below. The usual Sm-$C$ chevron structure, which we shall refer to as a nonplanar chevron, breaks the Sm-$A$ bookshelf structure in two ways. The cone angle tilt breaks the $y$-mirror symmetry (see Fig. 1). The layer buckling, by contrast, breaks the $z$-mirror symmetry. The two broken symmetries are in principle independent. However, they are linked energetically, because the layer deformation at the chevron tip favors some out-of-plane tilt. In addition, the surface anchoring biases the director toward an angle other than the preferred tilt. The onset of the chevron phase involves breaking both symmetries. However, they will not in general be broken at exactly the same temperature. This gives rise to some fine structure in the phase diagram close to the Sm-$A$–Sm-$C$ phase boundary which depends sensitively on the boundary conditions.

When the $y$-mirror symmetry breaks at higher temperatures than the $z$-mirror symmetry, the first phase transition is from Sm-$A$ to a bookshelf Sm-$C$ structure. The layers are not buckled, but the director is uniformly twisted with respect to the planar easy axis. When the temperature is further reduced, the conventional nonplanar chevron is recovered as the $z$-mirror symmetry also breaks. When it is the $z$-mirror symmetry which breaks first, a planar chevron structure is formed below the Sm-$A$–Sm-$C$ phase transition temperature. Again, at lower temperatures a nonplanar chevron occurs.

We restrict our studies to planar surface anchoring, in which the director is confined to the surface plane. We do, however, allow rotational freedom away from the easy axis in the surface plane. There are interesting phenomena associated with surface out-of-plane rotation [25–32], but we do not consider them here. The amount of rotation is governed by the strength of the orientational surface anchoring in the surface plane. This is the important control parameter in our study. We find that the Sm-$A$–Sm-$C$ bulk phase transition temperature is lowered for all finite surface orientational anchoring. At rather weak surface orientational anchoring, the first transition from the Sm-$A$ phase is to the bookshelf Sm-$C$ phase. At stronger surface orientational anchoring, the order of the phases is reversed in the fine structure of the phase boundary, and the first phase transition occurs from the Sm-$A$ to the planar chevron phase.

We may remark that symmetry breaking in the $y$-mirror plane can lead to bistability of the optical axis, whereas symmetry breaking in the $z$-mirror plane cannot by itself have this effect. This is a consequence of the interaction between the director and the optical polarization. Thus the nonplanar chevron and the bookshelf Sm-$C$ structures may be bistable. The planar chevron structure is not useful for electro-optical applications.

The plan of this paper is as follows. In Sec. II we introduce the model. In Sec. III we analytically estimate the threshold temperatures for the formation of the bookshelf, planar and nonplanar chevron structures. In Sec. IV we draw some brief conclusions.

## II. MODEL

In the Landau–de Gennes model the free energy of the Sm-$C$ liquid crystal cell is expressed by the local nematic director $\mathbf{n}$ and the complex smectic density wave $\psi(\mathbf{r}) = \eta(\mathbf{r})\exp\{i\phi(\mathbf{r})\}$, where $|\eta(\mathbf{r})|$ is the smectic order parameter and $\phi(\mathbf{r})$ is the phase factor determining the layer position. The normal to the layer is defined by $\boldsymbol{\nu}=\nabla\phi/|\nabla\phi|$. We shall study the structure close to the Sm-$A$–Sm-$C$ phase transition and far from the nematic-smectic phase transition. In that case it can be assumed that the smectic order parameter is constant and equal to its bulk value: $\eta(\mathbf{r})=\eta_B$.

The elastic free energy is written as a sum of the nematic and smectic contribution. In a one constant approximation for the nematic contribution, the free energy of the smectic phase is [21,24]

$$F=\tfrac{1}{2}K\int[(\nabla\cdot\mathbf{n})^2+(\nabla\times\mathbf{n})^2]d^3\mathbf{r} \tag{1}$$

$$+\int\{c_{\parallel}|(\mathbf{n}\cdot\nabla-iq_0)\psi|^2+c_{\perp}|(\mathbf{n}\times\nabla)\psi|^2$$

$$+D|(\mathbf{n}\times\nabla)^2\psi|^2\}d^3\mathbf{r}, \tag{2}$$

where Eq. (1) is the nematic elastic free energy, and Eq. (2) is the smectic elastic free energy. The constant $K$ is the nematic elastic constant, and $c_{\parallel}$, $c_{\perp}$, and $D$ are smectic elastic constants. The elastic constant $c_{\parallel}$ is related to the de Gennes compressibility constant $B$ [21]. The parameter $q_0$ is related to the layer thickness $d_0$ in the Sm-$A$ phase: $q_0=2\pi/d_0$. The elastic constant $c_{\perp}$ measures the energy associated with tilting the director away from the layer normal. It is temperature dependent: $c_{\perp}\propto(T-T_{AC})$ and $T_{AC}$ is the bulk phase transition temperature from the Sm-$A$ phase to the Sm-$C$ phase. The term with the elastic constant $D$ opposes the bending of the smectic layers. It also stabilizes an intermediate tilt of $\mathbf{n}$ with respect to the normal to the smectic layer in the Sm-$C$ phase.

To describe surface stabilized cells, a surface term has to be added to the free energy $F$. The surface energy is modeled by the following Rapini-Papoular terms:

$$F_S=-\tfrac{1}{2}W_S\int(\mathbf{n}\cdot\hat{\mathbf{z}})^2d^2\mathbf{r}+\tfrac{1}{2}\widetilde{W_S}\int(\mathbf{n}\cdot\hat{\mathbf{x}})^2d^2\mathbf{r}, \tag{3}$$

where $\hat{\mathbf{z}}$ is the easy axis in the surface plane, $\hat{\mathbf{x}}$ is the direction perpendicular to the surface plane, and $W_S$ and $\widetilde{W_S}$ are the anchoring strengths. We consider anchoring such that the director always lies in the surface plane. In this case, $\widetilde{W_S}\to\infty$. If, in addition, also $W_S\to\infty$, the director always aligns along the easy axis $\hat{\mathbf{z}}$. In the limit of no surface orientational anchoring ($W_S=0$) the director is free to choose the most favorable position in the surface plane.

This model can be modified to take into account more comprehensive surface treatments that favor finite pretilt. This is of technological importance, because depending on

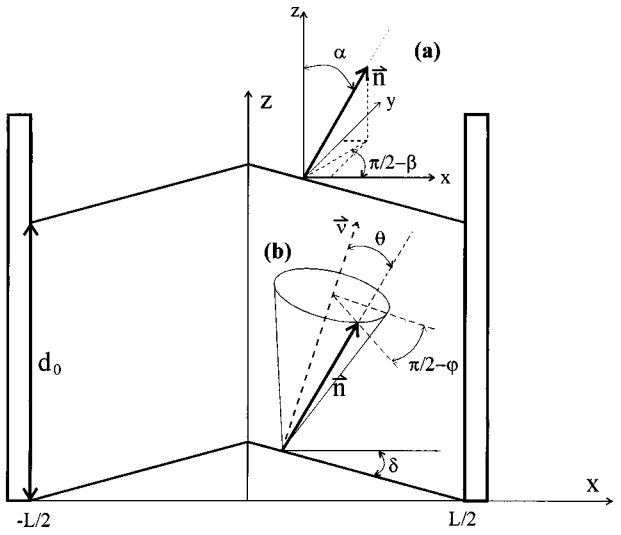


FIG. 2. (a) The coordinate system in which the numerical calculations were performed. (b) The coordinate system used to describe the chevron structure.

the surface pretilt two alignment structures $C_1$ and $C_2$ [25] can occur (Fig. 1). They can both coexist in a cell, and are separated by zigzag defects [26,27]. The effect of the surface pretilt angle on the stability of the $C_1$ and $C_2$ states was discussed in Refs. [28,29]. We shall not, however, address the problem of the stability of the $C_1$ and $C_2$ states in the present paper. With the surface treatment chosen here, the two structures are degenerate.

The coordinate systems used for the calculation and for the presentation of the results are shown in Fig. 2. The Sm-$C$ liquid crystal is confined between the plates located at $x=-L/2$ and $L/2$, as shown in Fig. 2(a). The layers are running in the $z$ direction. In the coordinate system chosen for numerical calculations the variables are the angles $\alpha$ and $\beta$, and the displacement vector $\mathbf{u}$. We assume that they are all functions of $x$ only. The smectic density wave enforces the periodicity in the $z$ direction, and is expressed as $\psi(\mathbf{r})=\eta_B \exp\{iq_0[z+u(x)]\}$. The displacement $u(x)$ describes departures from the planar layer configuration. The periodicity enforced in the $z$ direction is established in the Sm-$A$ phase and is $q_0=2\pi/d_0$.

The chevron structure is usually described in the local coordinate system by the molecular cone angle $\vartheta(x)$, the layer tilt angle $\delta(x)$, and the director rotation about the cone $\varphi(x)$ [Fig. 2(b)]. In the Landau–de Gennes model (2) the bulk value of the molecular cone angle $\vartheta_B$ in the Sm-$C$ phase ($c_\perp<0$) is expressed as $\tan\vartheta_B=\sqrt{-c_\perp/(2Dq_0^2)}$.

For computational purposes we write the nematic, smectic, and surface free energy densities in the dimensionless form. We use the dimensionless parameters

$$\mathcal{C}_\parallel=L^2/\lambda_\parallel^2, \quad \mathcal{C}_\perp=L^2/\lambda_\perp^2, \quad \text{and} \quad \mathcal{L}_S=L/\lambda_S, \tag{4}$$

where $\lambda_\parallel=[K/(c_\parallel q_0^2\eta_B^2)]^{1/2}$ and $\lambda_\perp=[K/(|c_\perp|q_0^2\eta_B^2)]^{1/2}$ are the correlation lengths, measuring the penetration of locally induced nematic bend or twist deformation into the smectic phase in the layer plane ($\lambda_\perp$) and along the layer normal ($\lambda_\parallel$); $\lambda_S=K/W_S$ is the surface extrapolation length. It is worth noticing that $\mathcal{C}_\parallel\propto c_\parallel$, $\mathcal{C}_\perp\propto|c_\perp|$ and $\mathcal{L}_S\propto W_S$.

It is also convenient to introduce the following dimensionless parameters:

$$\text{the reduced temperature: } t=T/T_{AC}-1, \tag{5}$$

$$\mathcal{C}_\perp/\mathcal{C}_\parallel=a_0|t|=(\lambda_\parallel/\lambda_\perp)^2, \tag{6}$$

$$D_1=Dq_0^4\eta_B^2L^2/K, \quad D_2=Dq_0^2\eta_B^2/K, \tag{7}$$

$$\rho=x/L, \quad w=du/dx. \tag{8}$$

A typical set of values of the dimensionless parameters is

$$\mathcal{C}_\parallel=10^5, \quad D_1=4\times10^4, \quad D_2=0.01, \quad a_0=1. \tag{9}$$

The choice of these values is discussed in the Appendix. The bulk value of the molecular cone angle expressed in terms of the dimensionless parameters is $\tan^2\vartheta_B=\mathcal{C}_\perp/(2D_1)$. The dimensionless free energy is defined as

$$G=\frac{L}{K}\frac{F+F_S}{S}=\int_{-1/2}^{1/2}g(\rho)d\rho+g_S(\rho=-\tfrac{1}{2})+g_S(\rho=\tfrac{1}{2}), \tag{10}$$

where $(F+F_S)/S$ is a free energy per unit of the surface, and $g(\rho)$ and $g_S(\rho)$ are the bulk and surface dimensionless free energy densities, respectively. The complete expressions for these quantities can be found in I.

In what follows we use the fact that close to the phase transition the variables $\alpha$, $\beta$, and $w$ are small: $\alpha,\beta,w\ll1$. In addition, $\beta$ can be set to zero everywhere in the cell. The reason for this is the following. The order parameter for the chevron structure is $w\neq0$, and $\alpha\neq0$ is the order parameter for the Sm-$C$ bookshelf phase. The angle $\beta$ is nonzero only when both $w$ and $\alpha$ are nonzero, and so to discuss the phase progression we can ignore it. This is the reason why we use $\alpha$, $\beta$, and $w$ as a set of variables for numerical calculations instead of $\vartheta$, $\delta$, and $\varphi$. The angle $\varphi$ can never be set to zero everywhere in the cell. It cannot even be assumed to be small.

With $\beta(\rho)=0$, $\alpha(\rho)\ll1$, and $w(\rho)\ll1$, we can reliably employ a Taylor series expansion of the free energy densities, where we include terms of up to the fourth order in $\alpha$ and $w$. The bulk dimensionless free energy density takes a simple form

$$g=-\mathcal{C}_\perp\alpha^2+\tfrac{1}{4}[\mathcal{C}_\parallel+4D_1]\alpha^4-\mathcal{C}_\perp w^2+D_1w^4+2D_1w^2\alpha^2 +D_2w_\rho^2+\tfrac{1}{2}\alpha_\rho^2, \tag{11}$$

where subscripts $\rho$ denote derivatives with respect to $\rho$. The dimensionless surface free energy density $g_S$ is

$$g_S(\rho)=-\tfrac{1}{2}\mathcal{L}_S(1-\alpha^2+\tfrac{1}{3}\alpha^4). \tag{12}$$

In addition, since $\widetilde{W_S}\to\infty$, $\beta$ is zero at both surfaces. We have chosen $\beta$ to be zero everywhere in the cell, so the boundary condition for $\beta$ is automatically satisfied.

Next we shall construct the expressions for the variables $\alpha$ and $w$. The order parameter $\alpha\neq0$ is associated with the breaking of the $y$-mirror symmetry. The variable $\alpha$ can be expressed as a Fourier series

$$\alpha(\rho)=\sum_{k=0}^{\infty}\alpha_k\cos(k\pi\rho), \tag{13}$$

where the fact that $\alpha$ is symmetric around the chevron tip was used. To see which terms dominate close to the temperature at which the $y$-mirror symmetry breaks, we examine the boundary condition for $\alpha$. It is (see I)

$$\left[\pm\frac{\partial g}{\partial\alpha_\rho}+\frac{\partial g_s}{\partial\alpha}\right]_{\rho=\pm 1/2}=0. \tag{14}$$

Using the expressions for the bulk and surface free energy densities (11) and (12) in the above boundary condition, we obtain

$$(\pm\alpha_\rho+\mathcal{L}_S\alpha)_{\rho=\pm 1/2}=0, \tag{15}$$

where a third order term in $\alpha$ has been neglected. When there is no surface orientational anchoring ($\mathcal{L}_S=0$), the first spatial derivative of $\alpha$ is zero at the surface, and near the temperature at which the $y$-mirror symmetry is broken $\alpha(\rho)$ can be approximated by $\alpha(\rho)=\alpha_0$. In the limit of infinitely strong surface orientational anchoring ($\mathcal{L}_S\to\infty$) $\alpha=0$ at both surfaces. So the correct ansatz for $\alpha$ is $\alpha(\rho)=\alpha_1\cos(\pi\rho)$. In general, at finite surface orientational anchoring neither $\alpha=0$ nor $\alpha_\rho=0$ at the surface, and the spatial dependence of $\alpha$ needs to be approximated by two terms in the Fourier series expansion: $\alpha(\rho)=\alpha_0+\alpha_1\cos(\pi\rho)$. However, we find that the calculations are a bit simpler if we use the following ansatz for $\alpha$, which is essentially the same as the one above:

$$\alpha(\rho)=\alpha_0\cos(\kappa\rho). \tag{16}$$

In the case of no orientational surface anchoring, $\kappa=0$, and in the limit of very strong anchoring, $\kappa=\pi$. The value of $\kappa$ at finite anchoring is obtained from the boundary condition (15):

$$\kappa\,\tan(\kappa/2)-\mathcal{L}_S=0. \tag{17}$$

This equation has to be solved numerically for a given $\mathcal{L}_S$.

To find the ansatz for $w(\rho)$ we use a similar procedure. The boundary condition for $w$ is

$$\left[\frac{\partial g}{\partial w_\rho}\right]_{\rho=\pm 1/2}=0, \tag{18}$$

from which it follows that

$$(w_\rho)_{\rho=\pm 1/2}=0. \tag{19}$$

The symmetric chevron structure requires that $w$ is antisymmetric around the chevron tip, and because of that $w$ must be zero at the chevron tip. The Fourier expansion of $w$ is thus

$$w(\rho)=\sum_{k=0}^{\infty}w_k\sin(k\pi\rho), \tag{20}$$

and the term that dominates close to the temperature at which the $z$-mirror symmetry breaks is

$$w(\rho)=w_1\sin(\pi\rho). \tag{21}$$

The harmonic approximations for $\alpha(\rho)$ and $w(\rho)$ are expected to be valid only for second order phase transition at which the $y$- and $z$-mirror symmetries break, respectively, and the amplitudes $\alpha_0$ and/or $w_1$ are small. That means that, in general, at temperatures at which a bookshelf Sm-$C$ structure deforms into a nonplanar chevron structure, the harmonic approximation for $\alpha(\rho)$ is not valid any more. Similarly, at temperatures at which a planar chevron structure deforms into a nonplanar one, the harmonic approximation for $w$ is not valid.

The correct ansatz for $w$ close to the planar-nonplanar chevron transition can easily be found directly from the free energy density (11) in the case of $\alpha(\rho)=0$. The free energy density is

$$g=-\mathcal{C}_\perp w^2+D_1w^4+D_2w_\rho^2, \tag{22}$$

and is minimal when the Euler-Lagrange equation

$$-\mathcal{C}_\perp w+2D_1w^3-D_2w_{\rho\rho}=0 \tag{23}$$

is satisfied together with the boundary condition $w_\rho|_{\rho=\pm 1/2}=0$ [see Eq. (19)]. The solution of this equation is $w=w_0\tanh(\rho/\lambda_w)$ with the amplitude $w_0=\sqrt{\mathcal{C}_\perp/(2D_1)}$ and the chevron width $\lambda_w=\sqrt{2D_2/\mathcal{C}_\perp}$. The boundary condition is satisfied if $\lambda_w\ll 1$, which is true at all temperatures except close to the onset of the planar chevron.

The ansatz for $w(\rho)$ close to the planar-nonplanar chevron transition is thus

$$w=w_0\tanh(\rho/\lambda_w),\quad w_0=\sqrt{\frac{\mathcal{C}_\perp}{2D_1}},\quad \lambda_w=\sqrt{\frac{2D_2}{\mathcal{C}_\perp}}. \tag{24}$$

There is no simple ansatz to be found for $\alpha(\rho)$ close to the bookshelf Sm-$C$–nonplanar chevron transition. In general the temperature for this transition can be found numerically by direct solution of the bulk Euler-Lagrange equations for $\alpha$ and $w$ together with the boundary conditions (15) and (19). It turns out, however, that for the chosen surface treatment the bookshelf Sm-$C$ structure can exist only in such a narrow temperature region that the harmonic approximation for $\alpha$ is still valid at the bookshelf Sm-$C$–nonplanar chevron transition.

## III. STRUCTURES CLOSE TO THE SM-$A$–SM-$C$ PHASE TRANSITION

The structures close to the Sm-$A$–Sm-$C$ phase transition are best presented by the $\lambda_S-|t|$ phase diagram (Fig. 3). All the transitions are second order. At stronger surface orientational anchoring the $z$ mirror symmetry breaks first, and a planar chevron structure (Fig. 4) is formed below the Sm-$A$–Sm-$C$ phase transition temperature $t_{\mathrm{plan}}$. This temperature is independent of the strength of the surface orientational anchoring. At lower temperatures the $y$-mirror symmetry breaks as well, and a nonplanar chevron structure (Fig. 5) is formed at $t<t_{\mathrm{CH}}$. At rather weak surface orientational anchoring ($\lambda_s\to\infty$) the $y$-mirror symmetry is broken at higher temperatures than the $z$-mirror symmetry, and a book-

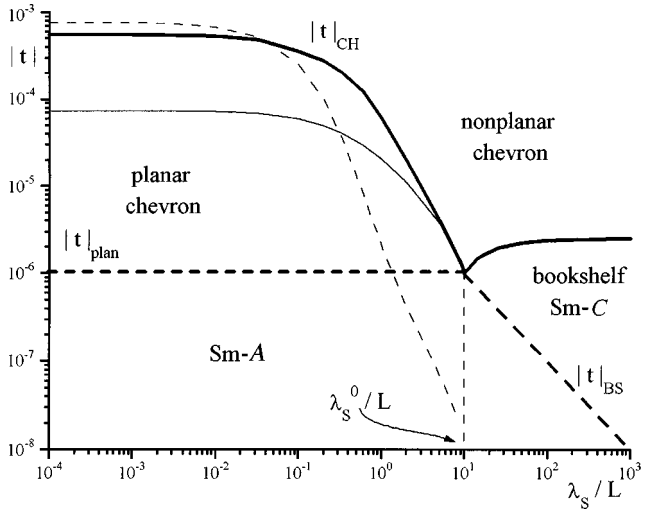


FIG. 3. Phase diagram, showing the stability areas of the bookshelf, planar chevron, and nonplanar chevron structures. At $\lambda_S < \lambda_S^0$ the thin full line presents the analytical estimate of $t_{CH}$ obtained with the harmonic approximation for $\alpha$ and $w$, and the dashed line presents the analytical estimate obtained by the harmonic approximation for $\alpha$ and a solitonlike approximation for $w$. The thick full line shows the numerically obtained transition temperature $t_{CH}$. At $\lambda_S > \lambda_S^0$, the numerically and analytically obtained transition temperatures agree well. Parameter values: $\mathcal{C}_\parallel = 10^5$, $D_1 = 4\times 10^4$, $D_2 = 0.01$, and $a_0 = 1$.

shelf Sm-$C$ structure (Fig. 6) is formed at $t < t_{BS}$. The latter deforms into a nonplanar chevron structure when temperature is further reduced and the $z$-mirror symmetry breaks as well. The $z$- and $y$-mirror symmetries are broken at the same temperature ($t = t_{plan}$) only at one specific surface extrapolation length $\lambda_S^0$.

In the following subsections we estimate analytically the transition temperatures between different structures. We compare these results with numerically obtained transition temperatures. By numerically obtained results we refer to the results obtained by numerical solution of the differential Euler-Lagrange equations (see I) obtained from the free energy density expression in which no simplifications were done [i.e., $\beta(\rho) \neq 0$ and, in general, $\alpha$, $\beta$, and $w$ are not a lot smaller than 1]. We shall first study two limiting cases: the case of infinitely strong anchoring ($\lambda_S = 0$) and the case on infinitely weak anchoring ($\lambda_S \to \infty$), and shall finally consider the case of finite anchoring.

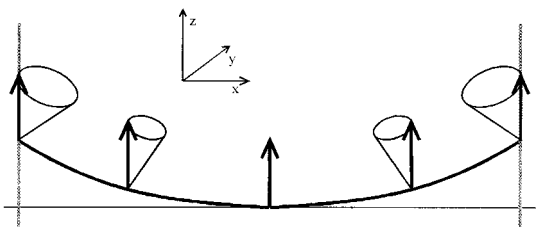


FIG. 4. Planar chevron structure. The director lies in the $xz$ plane. This structure is not optically bistable.

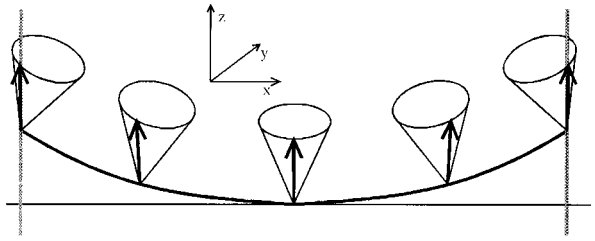


FIG. 5. Nonplanar chevron structure. At the chevron tip and at the surfaces, the director lies in the $yz$ plane.

### A. Infinitely strong anchoring ($\lambda_S = 0$)

#### *1. Sm-A→planar chevron*

At this transition $\alpha(\rho) = 0$ and for $w(\rho)$ the harmonic approximation (21) is used. The bulk free energy, obtained from Eqs. (10) and (11), is then

$$G = -\tfrac{1}{2}(\mathcal{C}_\perp - \pi^2 D_2) w_1^2 + \tfrac{3}{8} D_1 w_1^4. \tag{25}$$

The energy is minimal when the condition $\partial G/\partial w_1 = 0$ is satisfied. In this way we obtain the expression for the amplitude $w_1$:

$$w_1^2 = \frac{2}{3D_1}(\mathcal{C}_\perp - \pi^2 D_2). \tag{26}$$

The amplitude is real and different from zero if $\mathcal{C}_\perp > \pi^2 D_2$. Otherwise the energy is minimal with $w_1 = 0$ (bookshelf Sm-$A$ structure). It follows from Eq. (6) that $\mathcal{C}_\perp$ is temperature dependent. The reduced temperature at which the planar chevron structure is formed (i.e., the $z$-mirror symmetry breaks) is thus

$$|t|_{plan} = \frac{\pi^2 D_2}{a_0 \mathcal{C}_\parallel}. \tag{27}$$

By using a similar procedure and setting $w(\rho) = 0$ and $\alpha(\rho) = \alpha_0 \cos(\pi\rho)$, it can be shown that the $y$-mirror symmetry alone would break at $|t|_{BS} = \pi^2/(2a_0\mathcal{C}_\parallel)$. Since $D_2 \ll 1$ [see Eq. (9)], $|t|_{plan} < |t|_{BS}$ and the transition is Sm-$A$ → planar chevron not Sm-$A$ → bookshelf Sm-$C$.

It should be mentioned that in many circumstances the planar chevron structure occurs already in the Sm-$A$ phase, [33–36]. Since the change in the layer thickness is much smaller in the Sm-$A$ phase than in the Sm-$C$ phase, this effect can be ignored in the first approximation. So we have not considered it here.

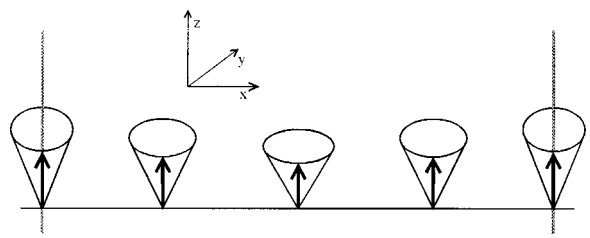


FIG. 6. Bookshelf Sm-$C$ structure. The director is tilted in the $yz$ plane everywhere in the cell.

#### 2. Planar chevron→nonplanar chevron

To estimate the temperature at which the planar chevron structure deforms into a nonplanar one, we use ansatz (24) for $w(\rho)$, and for $\alpha(\rho)$ we use the harmonic approximation (16) with $\kappa=\pi$. We calculate the free energy, minimize it over $\alpha_0$, thus find the amplitude $\alpha_0$, and finally we obtain the condition for $\alpha_0$ to be real:

$$\mathcal{C}_\perp - \tfrac{1}{2}\pi^2 - 2\mathcal{C}_\perp \int_{-1/2}^{1/2} \cos^2(\pi\rho)\tanh^2(\rho/\lambda_w)d\rho > 0. \tag{28}$$

The chevron tip width $\lambda_w$ is temperature dependent: $\lambda_w = \lambda_w(\mathcal{C}_\perp)$. The easiest way to estimate the critical temperature for the formation of the nonplanar chevron structure is to plot expression (28) as a function of $\mathcal{C}_\perp$, and estimate $(\mathcal{C}_\perp)^{\mathrm{CH}}$ at which expression (28) is zero from the plot. The reduced temperature at which a nonplanar chevron is formed is $|t|_{\mathrm{CH}} = (\mathcal{C}_\perp)^{\mathrm{CH}}/(a_0\mathcal{C}_\parallel)$.

### B. Zero anchoring ($\lambda_S\to\infty$)

#### 1. Sm-A→bookshelf Sm-C

At this transition $w(\rho)=0$ and $\alpha(\rho)=\alpha_0$ [see Eq. (16) with $\kappa=0$]. The free energy of the cell is

$$G = -\mathcal{C}_\perp\alpha_0^2 + \tfrac{1}{4}(\mathcal{C}_\parallel + 4D_1)\alpha_0^4, \tag{29}$$

and is minimized if

$$\alpha_0^2 = \frac{2\mathcal{C}_\perp}{\mathcal{C}_\parallel + 4D_1}. \tag{30}$$

The amplitude $\alpha_0$ is real if $\mathcal{C}_\perp \geqslant 0$. So the $y$-mirror symmetry breaks already at the Sm-$A$–Sm-$C$ bulk phase transition temperature: $t=0$.

#### 2. Bookshelf Sm-C→nonplanar chevron

It turns out that the bookshelf Sm-$C$ structure can exist only in such a narrow temperature region that the harmonic approximation for $\alpha(\rho)=\alpha_0$ can be used also at the bookshelf Sm-$C$–nonplanar chevron transition. For $w(\rho)$ we use the harmonic approximation (21). The following free energy density is obtained:

$$G = -\mathcal{C}_\perp\alpha_0^2 + \tfrac{1}{4}(\mathcal{C}_\parallel + 4D_1)\alpha_0^4 - \tfrac{1}{2}(\mathcal{C}_\perp - \pi^2 D_2)w_1^2 + D_1 w_1^2\alpha_0^2 + \tfrac{3}{8}D_1 w_1^4. \tag{31}$$

The energy is minimal when the amplitudes $\alpha_0$ and $w_1$ take the values

$$\alpha_0^2 = \frac{2\mathcal{C}_\perp - 2D_1 w_1^2}{\mathcal{C}_\parallel + 4D_1} \tag{32}$$

and

$$w_1^2 = \frac{2}{3D_1}(\mathcal{C}_\perp - \pi^2 D_2 - 2D_1\alpha_0^2). \tag{33}$$

The $z$-mirror symmetry is broken when at finite $\alpha_0$ the amplitude $w_1$ becomes real. We find that the condition $w_1^2 \geqslant 0$ is satisfied at temperatures lower than $t_{\mathrm{CH}}$, where

$$|t|_{\mathrm{CH}} = \frac{\pi^2 D_2(1 + 4D_1/\mathcal{C}_\parallel)}{\mathcal{C}_\parallel a_0}. \tag{34}$$

For a given set of parameters (9), this temperature is $2.6\times10^{-6}$, which is small enough that the harmonic approximation for $\alpha(\rho)$ is still valid at this transition point.

### C. Finite anchoring

#### 1. Sm-A→bookshelf Sm-C or planar chevron

With the harmonic expression (16) for $\alpha$ and $w$ set to zero the free energy of the bookshelf structure is obtained from Eq. (10):

$$G = \frac{\mathcal{C}_\parallel + 4D_1}{4}\alpha_0^4 \int_{-1/2}^{1/2} \cos^4(\kappa\rho)d\rho - \frac{1}{2}(2\mathcal{C}_\perp + \kappa^2)\alpha_0^2 \int_{-1/2}^{1/2} \cos^2(\kappa\rho)d\rho + \frac{1}{2}\kappa^2\alpha_0^2 - \mathcal{L}_S + \mathcal{L}_S\alpha_0^2\cos^2(\kappa/2) - \frac{1}{3}\mathcal{L}_S\alpha_0^4\cos^4(\kappa/2). \tag{35}$$

It can easily be found that the amplitude $\alpha_0$, which minimizes the above free energy (35), is real when $t<t_{\mathrm{BS}}$, where

$$|t|_{\mathrm{BS}} = \frac{\kappa^2}{2a_0\mathcal{C}_\parallel}. \tag{36}$$

At infinitely small surface anchoring ($\mathcal{L}_S=0$ and $\kappa=0$) the temperature $t_{\mathrm{BS}}=0$, the result which we have already obtained in Sec. III B 1. At finite surface orientational anchoring the Sm-$A$–Sm-$C$ phase transition temperature is lowered from its bulk value $t=0$ to $t_{\mathrm{BS}}<0$. The Sm-$C$ bookshelf structure is inhomogeneous since $\alpha(\rho)=\vartheta(\rho)=\alpha_0\cos(\kappa\rho)$.

The Sm-$A$–planar chevron transition can occur at $|t|_{\mathrm{plan}} = \pi^2 D_2/(a_0\mathcal{C}_\parallel)$. This temperature is independent of the surface orientational anchoring strength, and has already been found in Sec. III A 1.

If $t_{\mathrm{plan}} > t_{\mathrm{BS}}(\mathcal{L}_S)$, the $z$-mirror symmetry breaks first when the Sm-$A$ phase is cooled down to the Sm-$C$ phase, and a planar chevron structure is formed. If $t_{\mathrm{BS}} > t_{\mathrm{plan}}$ the $y$-mirror symmetry breaks first, and a bookshelf Sm-$C$ structure is formed. Both symmetries are broken at the same temperature at that strength of the surface orientational anchoring ($\mathcal{L}_S^0$) where $t_{\mathrm{BS}}(\mathcal{L}_S^0) = t_{\mathrm{plan}}$:

$$\kappa_0^2 - 2\pi^2 D_2 = 0. \tag{37}$$

The parameter $\kappa_0$ is related to $\mathcal{L}_S^0$ by the boundary condition (17). So it follows from the above expression (37) that the value of $\mathcal{L}_S^0$ depends only on the value of $D_2$.

#### 2. Bookshelf Sm-C→nonplanar chevron

With the use of the harmonic expressions (21) and (16) for the variables $\alpha$ and $w$ and the expressions for the bulk

(11) and surface (12) free energy densities we obtain the following free energy from (10):

$$G=A_1\alpha_0^2+A_2\alpha_0^4+A_3w_1^2+A_4w_1^4+A_5\alpha_0^2w_1^2. \quad (38)$$

The factors $A_i$ $(i=1,\ldots,5)$ are

$$A_1=-\tfrac{1}{2}(2\mathcal{C}_\perp+\kappa^2)I_1+\tfrac{1}{2}\kappa^2+\mathcal{L}_S\cos^2(\kappa/2), \quad (39)$$

$$A_2=\tfrac{1}{4}(\mathcal{C}_\parallel+4D_1)I_2-\tfrac{1}{3}\mathcal{L}_S\cos^4(\kappa/2), \quad (40)$$

$$A_3=-\tfrac{1}{2}(\mathcal{C}_\perp-\pi^2D_2), \quad (41)$$

$$A_4=\tfrac{3}{8}D_1, \quad (42)$$

$$A_5=2D_1I_3, \quad (43)$$

with

$$I_1=\int_{-1/2}^{1/2}\cos^2(\kappa\rho)d\rho, \quad (44)$$

$$I_2=\int_{-1/2}^{1/2}\cos^4(\kappa\rho)d\rho, \quad (45)$$

$$I_3=\int_{-1/2}^{1/2}\sin^2(\pi\rho)\cos^2(\kappa\rho)d\rho. \quad (46)$$

The amplitudes $\alpha_0$ and $w_1$ that minimize the free energy (38) are

$$\alpha_0^2=\frac{1}{2A_2}[-A_1-A_5w_1^2] \quad (47)$$

and

$$w_1^2=\frac{-A_3-A_5\alpha_0^2}{2A_4}. \quad (48)$$

The reduced temperature $|t|_{\mathrm{CH}}$ is found by requiring that the amplitude $w_1$ is real (i.e., $w_1^2\geqslant 0$) at finite $\alpha_0$. At the transition point $w_1^2=0$ and $\alpha_0^2=-A_1/(2A_2)$ (that is the value of $\alpha_0$ in the bookshelf structure). From Eq. (48), we thus obtain that the amplitude $w_1$ is real if $-A_3+A_5A_1/(2A_2)>0$. Factors $A_1$ and $A_3$ depend linearly on the reduced temperature $|t|$, and from the above expression $|t|_{\mathrm{CH}}$ can be determined. The results agree well with the numerically obtained transition temperatures.

From the phase diagram in Fig. 3, we estimate that the maximum reduced temperature region in which the equilibrium bookshelf Sm-$C$ structure can exist is at zero surface anchoring and is approximately $3\times10^{-6}$. With $T_{AC}\sim 300$ K, this gives a temperature region of the order of $10^{-3}$ K. Things can be different if one boundary allows relatively free motion of the molecules along the alignment direction. In Ref. [37], it was shown that in a ferroelectric liquid crystal cell with antiparallel surface tilt cooling into the Sm-$C$ phase did not produce the expected chevron structure. A tilted bookshelf structure was formed instead.

#### *3. Planar chevron→nonplanar chevron*

Now we use ansatz (24) for $w(\rho)$ and ansatz (16) for $\alpha(\rho)$. The free energy of the cell is then

$$G=B_1\alpha_0^2+B_2\alpha_0^4+G_{\mathrm{plan}}, \quad (49)$$

where $G_{\mathrm{plan}}$ is the free energy of a planar chevron structure and the factors $B_1$ and $B_2$ are

$$B_1=A_1+\mathcal{C}_\perp\int_{-1/2}^{1/2}\cos^2(\kappa\rho)\tanh^2(\rho/\lambda_w)d\rho, \quad (50)$$

$$B_2=A_2. \quad (51)$$

We minimize the free energy and obtain the amplitude $\alpha_0$:

$$\alpha_0^2=\frac{-B_1}{2B_2}. \quad (52)$$

This amplitude is real when

$$B_1\leqslant 0, \quad (53)$$

from where the planar chevron–nonplanar chevron transition temperature follows.

In Fig. 3 we compare the temperature $|t|_{\mathrm{CH}}$ obtained in this way with the one obtained numerically. The temperatures agree well at very strong surface orientational anchorings, where the temperature of the nonplanar chevron formation is low enough that the approximation $\lambda_w\ll 1$ [and thus the ansatz (24) for $w(\rho)$] is valid. However, close to the surface orientational anchoring strength $\mathcal{L}_S^0$, the planar-nonplanar chevron transition temperature is so high that the condition $\lambda_w\ll 1$ is not satisfied.

At anchorings close to $\mathcal{L}_S^0$ we use the harmonic ansatz (21) for $w(\rho)$. The temperature $|t|_{\mathrm{CH}}$ can be found from expressions (47) and (48) which were obtained in Sec. III C 2. Now we seek the condition $\alpha_0^2\geqslant 0$ at finite $w_1$. The reduced temperature $|t|_{\mathrm{CH}}$ is found by setting $w_1^2=-A_3/(2A_4)$ (the value in a planar chevron) and putting this in Eq. (47), where we require $\alpha_0^2=0$. We obtain the condition $-A_1+A_5A_3/(2A_4)=0$, from which $|t|_{\mathrm{CH}}$ is determined. It can be seen from Fig. 3 that this approximation gives good agreement with the numerical result at the anchorings close to $\mathcal{L}_S^0$.

The maximum reduced temperature region in which a planar chevron can exist can be deduced from the phase diagram in Fig. 3. At very strong surface anchoring ($\lambda_S\to 0$) the reduced temperature region is of the order of $10^{-3}$. With $T_{AC}\sim 300$ K this gives a temperature region of the order of $10^{-1}$ K.

The temperature regions of the planar chevron and the bookshelf Sm-$C$ structure are very narrow. The mean field free energies do not include fluctuations which may affect the stability of phases which only exist within a narrow temperature window. As a result, the phase topology predicted by the mean field theory may be unreliable. Here we check this possibility using estimates of energy determined from equipartition. Specifically, we have compared the amplitudes of the relevant order parameter fluctuations with the order 1parameter amplitudes $\alpha_0$ (in the bookshelf phase) and $w_1$ (in the planar chevron) which have been obtained using the mean field theory.

We first discuss the bookshelf Sm-$C$ phase. We calculate $\langle \Delta\alpha^2 \rangle$ assuming only nematic fluctuations; the smectic layer will distort with the director, and deviations of the director from the smectic normal can be neglected. Then for $q_x \sim 1/L$ the amplitude of the fluctuations can be estimated as [38]

$$\langle \Delta\alpha^2 \rangle \sim k_B T/(LK) \sim 10^{-4},$$

where the values $T \sim 300$ K, $L = 2\ \mu$m, and $K \sim 10^{-11}$ J/m were used. We consider the mean field value of $\alpha_0^2$ at its largest value, which is most favorable to the mean field theory. This occurs at the bookshelf Sm-$C$–nonplanar chevron transition in the limit of zero surface anchoring. In this situation

$$\alpha_0^2 \sim 10^{-6},$$

as follows from Eq. (30) if we take for $\mathcal{C}_\perp = 0.26$, i.e., the value at the bookshelf Sm-$C$–nonplanar chevron transition (see Fig. 3), and for other parameters we use the values given in Eq. (9). We may conclude that since $\langle \Delta\alpha^2 \rangle / \alpha_0^2 > 1$ in the putative bookshelf Sm-$C$ phase, this phase may well not be stable.

We now discuss the planar chevron. The fluctuations of the layer displacement are given by [38]

$$\langle \Delta w^2 \rangle \sim k_B T/(B\lambda_\parallel^2 L) \sim 10^{-4},$$

where $B$ is the de Gennes layer compressibility constant which is related to $\lambda_\parallel$ by the relation $\lambda_\parallel = \sqrt{K/B}$. Adopting an analogous procedure to that adopted above, we consider the mean field amplitude $w_1$ where it is largest. This occurs at the planar-nonplanar chevron transition in the limit of infinite surface anchoring. At this point in the phase diagram, $w_1$ is given by Eq. (24). At the planar-nonplanar chevron transition $\mathcal{C}_\perp \sim 10^2$ (see Fig. 3), and using the values (9) for other parameters, we can estimate

$$w_1^2 \sim 10^{-3}.$$

Thus, by contrast with the bookshelf Sm-$C$ phase, the planar chevron phase does seem stable with respect to fluctuations, at least in the limit of sufficiently strong surface orientational anchorings. This result is sensible because planar chevron structure has been observed in Sm-$A$ chevron cells [33,34].

## IV. CONCLUSIONS

We have used the Landau–de Gennes model to study analytically the conditions for the formation of the symmetric chevron in a surface stabilized Sm-$C$ liquid crystal cell. A simple Rapini-Papoular surface anchoring term has been used. The model can be generalized to consider a more complex set of assumptions. We find that upon cooling the Sm-$A$ liquid crystal to the Sm-$C$ phase three different structures can occur, depending on the strength of the surface orientational anchoring and the ratio among the material constants. Far from the nematic-smectic phase transition, the following two schemes are possible. If the surface anchoring is strong enough the Sm-$A$–Sm-$C$ phase transition temperature is lowered from $T_{AC}$ to $T_{\rm plan}$. At $T < T_{\rm plan}$ a planar chevron structure is formed. This structure is stable until $T = T_{\rm CH}$. Below $T_{\rm CH}$, a nonplanar chevron structure is formed. When the surface orientational anchoring is weak enough, the Sm-$A$–Sm-$C$ phase transition is lowered to $T_{\rm BS}$. Below this temperature a bookshelf Sm-$C$ structure is formed. When temperature is further reduced a bistable chevron structure is formed below $T_{\rm CH}$. The critical strength of the surface orientational anchoring that divides the two possible schemes is rather low. So in most realistic cases we probably have the transition from Sm-$A$ to a planar chevron structure and then to a nonplanar chevron structure. The temperature range in which the planar chevron structure is stable is at most $10^{-1}$ K for typical materials. The temperature range in which the equilibrium bookshelf structure exists at very weak surface anchoring is of the order of $10^{-3}$ K. The stability region of the bookshelf structure is very narrow, so this phase might disappear due to fluctuations in the nematic director. As a result of the narrow temperature range in which the planar chevron structure can exist, we conclude that in most experimental cases only a nonplanar chevron structure needs to be considered.

## ACKNOWLEDGMENTS

N.V. thanks Primož Ziherl and Samo Kralj for useful discussions.

## APPENDIX: THE CHOICE OF THE MATERIAL CONSTANTS

Typical values of the parameters entering the model are $L \approx 2\ \mu$m and $d_0 \sim \lambda_\parallel \approx 3$ nm [38,39]. The values of $c_\perp$, $c_\parallel$, and $D$ have been measured close to the $N$–Sm-$A$–Sm-$C$ multicritical point [40]. From those measurements of $|c_\perp|/c_\parallel$ at different $|t|$, we estimate that $a_0 \sim o(1)$. Far from the Sm-$A$–Sm-$C$ phase transition temperature, we use McMillan's [41] estimate that $a_0|t|$ is of the order of the ratio between the molecular diameter and the molecular length, and we take $a_0|t| \approx 0.1$. The parameter $D_1$ is calculated using the values for $a_0|t|$ and $\lambda_\parallel$, and assuming a value for the bulk molecular cone angle. For the materials showing the $N$–Sm-$A$–Sm-$C$ phase transition $\vartheta_B \approx 20°$ far from the Sm-$A$–Sm-$C$ phase transition temperature. $D_2$ is obtained from $D_1$ by noting that $D_2 = D_1/(L^2 q_0^2)$.

[1] T. P. Rieker, N. A. Clark, G. S. Smith, D. S. Parmer, E. B. Sirota, and C. R. Safinya, Phys. Rev. Lett. **59**, 2658 (1987).
[2] Y. Ouchi, J. Lee, H. Takes, A. Faked, K. Condo, T. Kitamura, and A. Mukoh, Jpn. J. Appl. Phys. **27**, L725 (1988).
[3] J. E. Maclennan, M. A. Handshy, and N. A. Clark, Liq. Cryst. **7**, 787 (1990).
[4] P. C. Willis, N. A. Clark, and C. R. Safinya, Liq. Cryst. **11**, 581 (1992).
[5] S. J. Elston, Liq. Cryst. **9**, 769 (1991).
[6] S. J. Elston and J. R. Sambles, Ferroelectrics **113**, 325 (1991).
[7] C. Lavers and J. R. Sambles, Ferroelectrics **113**, 339 (1991).
[8] S. J. Elston and J. R. Sambles, Mol. Cryst. Liq. Cryst. **200**, 167 (1991).
[9] M. Brunet and Ph. Martinot-Lagarde, J. Phys. II **6**, 1687 (1996).
[10] M. Cagnon and G. Durand, Phys. Rev. Lett. **70**, 2742 (1993).
[11] N. A. Clark, T. P. Rieker, and J. E. Maclennan, Ferroelectrics **85**, 79 (1988).
[12] J. E. Maclennan, M. A. Handshy, and N. A. Clark, Liq. Cryst. **7**, 787 (1990).
[13] M. Nakagawa and T. Akahane, J. Phys. Soc. Jpn. **55**, 1516 (1986).
[14] M. Nakagawa, Displays **11**, 67 (1990).
[15] J. Sabater, J. M. S. Pena, and J. M. Otón, J. Appl. Phys. **77**, 3023 (1995).
[16] A. De Meyere, H. Pauwels, and E. De Ley, Liq. Cryst. **14**, 1269 (1993).
[17] A. De Meyere and I. Dahl, Liq. Cryst. **17**, 379 (1994).
[18] L. Limat, J. Phys. II **5**, 803 (1995).
[19] L. Le Bourhis and L. Dupont, Mol. Cryst. Liq. Cryst. **275**, 155 (1996).
[20] M. Brunet and L. Lejček, Liq. Cryst. **19**, 1 (1995).
[21] N. Vaupotič, S. Kralj, M. Čopič, and T. J. Sluckin, Phys. Rev. E **54**, 1 (1996).
[22] P. G. de Gennes, Solid State Commun. **10**, 753 (1972).
[23] J. Chen and T. C. Lubensky, Phys. Rev. A **14**, 1202 (1976).
[24] T. C. Lubensky and S. R. Renn, Phys. Rev. A **41**, 4392 (1990).
[25] J. Kanbe, H. Inoue, A. Mizutome, Y. Hanyuu, K. Katagiri, and S. Yoshihara, Ferroelectrics **114**, 3 (1991).
[26] M. A. Handshy and N. A. Clark, Ferroelectrics **59**, 69 (1984).
[27] N. A. Clark and T. P. Rieker, Phys. Rev. A **37**, 1053 (1988).
[28] D. C. Ulrich and S. J. Elston, Ferroelectrics **178**, 177 (1996).
[29] J. C. Jones, Ferroelectrics **178**, 155 (1996).
[30] S. Kralj and S. Žumer, Phys. Rev. E **54**, 1610 (1996).
[31] J. Xue, Proc. SPIE **2892**, 10 (1996).
[32] P. Watson, P. J. Bos, and J. Pirš, Phys. Rev. E **56**, R3769 (1997).
[33] Y. Takanishi, Y. Ouchi, H. Takezoe, and A. Fukuda, Jpn. J. Appl. Phys. **28**, L487 (1989).
[34] Y. Ouchi, Y. Takanishi, H. Takezoe, and A. Fukuda, Jpn. J. Appl. Phys. **28**, 2547 (1989).
[35] L. Limat and J. Prost, Liq. Cryst. **13**, 101 (1993).
[36] S. Kralj and T. J. Sluckin, Phys. Rev. E **48**, 3244 (1994).
[37] L. Z. Ruan, J. R. Sambles, and J. Seaver, Liq. Cryst. **21**, 909 (1996).
[38] P. G. de Gennes and J. Prost, *The Physics of Liquid Crystals* (Clarendon, Oxford, 1993).
[39] M. S. Turner, M. Maaloum, D. Ausserré, J.-F. Joanny, and M. Kunz, J. Phys. II **4**, 689 (1994).
[40] L. J. Martinez-Miranda, A. R. Kortan, and R. J. Birgeneau, Phys. Rev. Lett. **56**, 2264 (1986).
[41] W. L. McMillan, Phys. Rev. A **7**, 1673 (1973).